Impact of unbalanced charge transport on the efficiency of normal and inverted solar cells

Kotlarski, J. D.; Blom, P. W. M.

Published in:
Applied Physics Letters

DOI:
10.1063/1.3663860

Publication date:
2012

Impact of unbalanced charge transport on the efficiency of normal and inverted solar cells

J. D. Kotlarski[1] and P. W. M. Blom[1,2,a)]
[1]*Zernike Institute for Advanced Materials, University of Groningen, Nijenborgh 4, 9747 AG Groningen, The Netherlands*
[2]*TNO/Holst Centre, High Tech Campus 31, P.O. Box 8550, 5605 KN Eindhoven, The Netherlands*

(Received 2 August 2011; accepted 19 October 2011; published online 5 January 2012; corrected 17 January 2012)

In a normal solar cell, most charge carriers are generated close to the anode, such that electrons have to travel a longer distance as compared to the holes. In an inverted solar cell, holes have to travel a longer distance. We use a combined optical and electronic model to simulate the effect of unbalanced transport on the efficiency of normal and inverted single and tandem solar cells. When the electrons are ten times more mobile than the holes, the efficiency for a single cell with a thickness of 250 nm drops from 7.5% to 4.5% when changing from a normal to an inverted structure. For opposite mobility ratio, the inverted structure clearly outperforms the normal structure. © *2012 American Institute of Physics*. [doi:10.1063/1.3663860]

In recent years, organic solar cell performance has been pushed beyond a power conversion efficiency (*PCE*) of 7% by improvements on materials, solar cell design, and manufacturing.[1,2] The common device structure for polymer based organic solar cells utilizes indium tin oxide (ITO) covered by poly(3,4-ethylene dioxythiophene) [PEDOT] doped with poly(4-styrenesulfonate) [PSS] as a transparent anode, followed by a photoactive polymer:fullerene blend and finally a suitable reflective cathode on top of it. A drawback of this normal device structure is that the ITO\PEDOT:PSS interface is unstable and diminishes organic solar cell performance over time.[3,4] One way of overcoming this drawback is to invert the structure of the device, so that an electrically conductive and transparent cathode is placed on the ITO and on top of the active material a suitable reflective anode, which has been implemented in recent years.[5–13] For both device structures, the incoming light is reflected at the reflective end electrode, leading to a pattern of self-interfering light in the device. For sufficiently thin active layers (<200 nm), this results in the majority of photons being absorbed near the transparent electrode, generating most of the charge carriers in that region.[14–17] However, when the charge transport in the solar cell is unbalanced, the slowest charge carriers either will have to travel to the transparent electrode or to the reflective electrode, depending on the device geometry. In the latter case, the average travel distance and time are relatively long, thus enhancing space charge buildup and related losses and thereby decreasing device performance.[15,18] In this study, we use combined optical and electrical modeling to simulate normal and inverted single and tandem solar cell devices with unbalanced transport.

As a first step, we simulate single solar cells using a recently developed combined optical and electrical model.[14–17,19] A typical device stack is simulated and consists of a silica substrate of 0.75 mm thickness with on top of it a 130 nm thick layer of ITO. In the case of a normal device structure, the ITO layer is covered with a 40 nm thick layer of PEDOT:PSS as transparent anode, a layer of the polymer:-fullerene bulk heterojunction blend as active layer with varying thickness, and 1 nm of lithium fluoride (LiF) topped with 100 nm of aluminium (Al) as reflective cathode. In the case of an inverted device structure, on top of the ITO layer, a 20 nm thick layer of zinc oxide (ZnO) as transparent cathode is used, then the polymer:fullerene bulk heterojunction blend as active layer, a 10 nm thick layer of molybdenum trioxide (MoO_3) as transparent anode covered with a 100 nm thick layer of Al as reflective electric contact. Necessary for simulating the optical performance of these devices are the optical properties of the materials. Those of MoO_3 and Al are taken from literature,[20,21] those of silica, ITO, PEDOT:PSS, ZnO, and LiF were determined with a Woollam variable-angle spectroscopic ellipsometer (VASE) by variable angle ellipsometry. The optical properties of the polymer:fullerene blend have been previously used,[22] with the blend consisting of a polymer:fullerene mixture in a 2 to 1 volumetric ratio for a polymer band gap of 1.7 eV.[22] In the simulations, the thickness of the active layer is varied between 10 and 250 nm in steps of 10 nm. For the electrical part of the modeling, we take the energy levels of the lowest unoccupied molecular orbital (LUMO) and the highest occupied molecular orbital (HOMO) of the fullerene to be 3.8 and 6.1 eV and of the polymer to be 3.5 and 5.2 eV, respectively. With a typical loss of 0.6 eV with respect to the optical bandgap,[23] an open circuit voltage V_{oc} of typically 1 eV is used. Further electronic parameters of the active layer used in the electronic device model are temperature $T = 295$ K, relative dielectric constant $\varepsilon_r = 3.4$, charge pair separation $a = 1.8$ nm, and bound e-h pair decay rate $k_f = 2 \times 10^4\ s^{-1}$, being similar to slowly dried poly(3-hexylthiophene and [6,6]-phenyl-C61-butyric acid methyl ester (P3HT:PCBM) cell parameters.[24] The electron and hole mobilities $\mu_{e,h}$ are varied between 10^{-10}, 10^{-9}, 10^{-8}, and 10^{-7} m^2/Vs, with the latter being an optimum value.[24] The ratio between μ_e and μ_h, μ_e/μ_h, is varied between 0.001 and 1000 in scale steps of 10, with the highest mobility being fixed at the optimum value of 10^{-7} m^2/Vs. In

a)Author to whom correspondence should be addressed. Electronic mail: paul.blom@tno.nl.

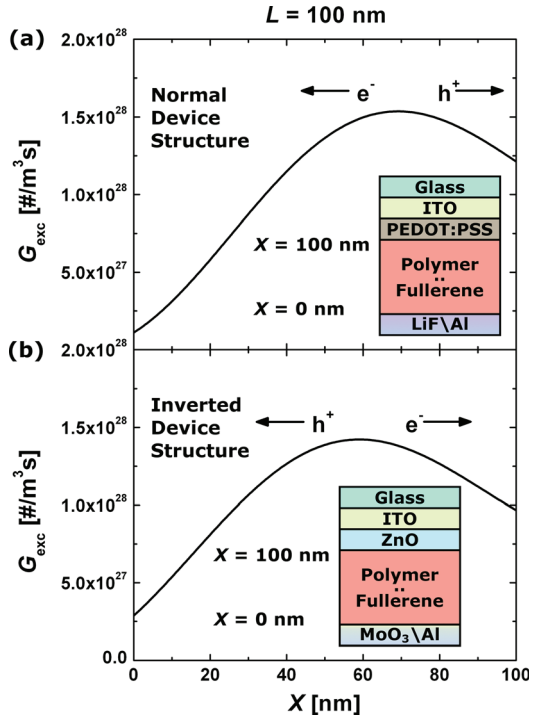

FIG. 1. (Color online) Optical absorption rate G_{exc} showing the absorption profile of two 100 nm thick active layers in normal (a) and inverted (b) single device structures. X denotes the distance from the boundary between the active layer and the reflective electrode. Note the small shift of the absorption profile for the two different device structures.

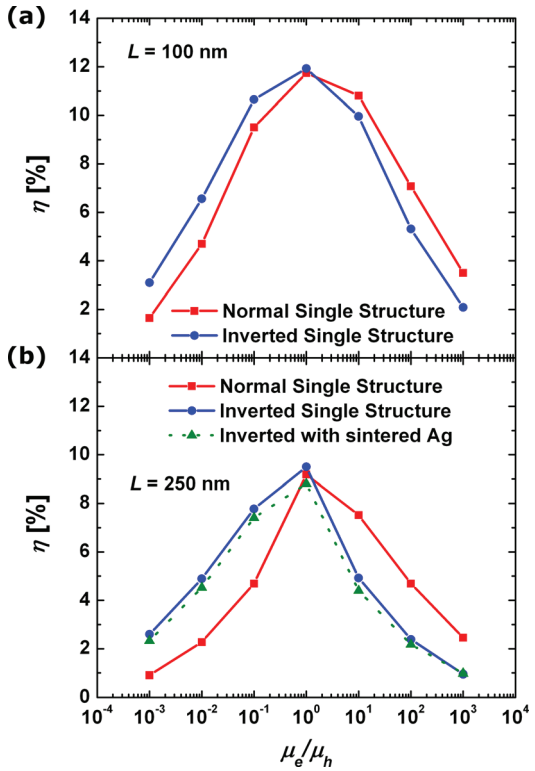

FIG. 2. (Color online) Power conversion efficiency η for different electron and hole mobility ratios μ_e/μ_h of normal and inverted single device structures for an active layer thickness L of 100 nm (a) and 250 nm (b). In (b) there is an additional set of simulated data for inverted devices with a less reflective printed and subsequently sintered Ag electrode. Note that the performance difference between normal and inverted devices for unbalanced charge transport is significantly bigger for 250 nm thick devices than 100 nm thick ones.

this way, the effect of unbalanced transport for the normal and inverted device configuration can be visualized as a function of the μ_e/μ_h ratio.

In Fig. 1, the optical absorption profile of a device with a 100 nm thick active layer is shown for both device structures. The expected maximum of absorption due to interference is observed as well as the typical quadratic like increase in absorption near the reflective electrode. As expected, the majority of charge carriers is generated near the active layer's side of light influx, independent of device structure. Furthermore, it appears that the total absorbed flux of the normal and inverted device are very similar.

As a next step, we compare the electrical performance of single solar cells with normal or inverted device structures as a function of μ_e/μ_h for active layer thicknesses of 100 (Fig. 2(a)) and 250 nm (Fig. 2(b)), respectively. As expected for unbalanced charge transport, the overall performance of the devices becomes worse for increasing or decreasing μ_e/μ_h, clearly showing the detrimental effects of increased space charge buildup and recombination on the device performance. From Fig. 2(a), it is observed that for a 100 nm thick solar cell the device performance already drops significantly from the calculated 12% efficiency for a fully optimized device to almost 10% for devices with the slowest charge carriers having a 10 times lower mobility than the fastest ones. Furthermore, when electrons are the slowest charge carriers, the inverted device structure has the best performance, which is usually the case for polymer:polymer devices. When holes are the slowest charge carriers, the normal device structure has the best performance, which is the case for most polymer:fullerene devices. In that case, a change from normal to inverted geometry would lead to an efficiency loss from 11% to 10%. For large-area, roll-to-roll processed solar cell devices with a 250 nm active layer are far more attractive due to an improved homogeneity of the layer thickness and improved robustness for electrical shorts, leading to a higher production yield. However, for this thicker layer, the distances that the slowest carriers have to travel become larger, making the effects of unbalanced charge transport even more pronounced. As shown in Fig. 2(b), when the holes are ten times slower than the electrons, the efficiency drops from 7.5% to 4.5%, when changing from a normal to an inverted device. In case that the holes are ten times faster than the electrons, the inverted solar cell has a calculated efficiency of 8% compared to an efficiency of only 5% for the normal cell.

To achieve higher efficiencies, a lot of attention has recently been paid to tandem solar cells.[25] Also, here a choice between a normal or inverted device structure can be made. The normal tandem structure is build up as follows: A 0.75 mm silica substrate with on top of it a 130 nm thick layer of ITO as transparent electric contact, a 40 nm thick layer of PEDOT:PSS as transparent anode, a variably thick layer of polymer:fullerene bulk heterojunction blend as back active layer, a 20 nm thick layer of ZnO as transparent cathode, a 40 nm thick layer of neutralized PEDOT:PSS as transparent anode, a variably thick layer of polymer:fullerene bulk heterojunction blend as back active layer, and a 1 nm thick layer of LiF and a 100 nm thick layer of Al as reflective cathode.[5,26] The inverted tandem is structured as follows: A

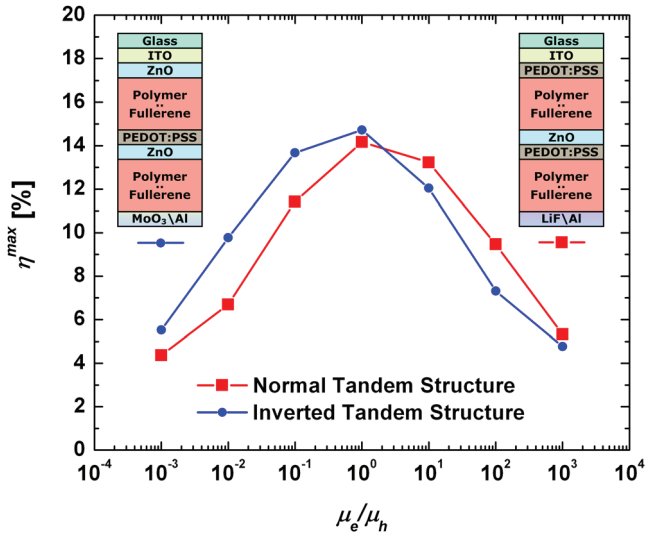

FIG. 3. (Color online) Optimized power conversion efficiency η^{max} for different electron and hole mobility ratios μ_e/μ_h of normal and inverted tandem device structures. Note that for μ_e/μ_h = 0.001 and 1000 the difference in η^{max} for normal and inverted device structures is significantly smaller than for single devices.

0.75 mm silica substrate with on top of it a 130 nm thick layer of ITO as transparent electric contact, a 20 nm thick layer of ZnO as transparent cathode, a variably thick layer of polymer:fullerene bulk heterojunction blend as front active layer, a 40 nm thick layer of PEDOT:PSS as transparent anode, a 20 nm thick layer of ZnO as transparent cathode, a variably thick layer of polymer:fullerene bulk heterojunction blend as back active layer, a 10 nm thick layer of MoO_3 as transparent anode, and a 100 nm thick layer of Al as reflective electric contact. The front and back active layers, however, have now different optical and electrical characteristics, as the optimized polymer band gaps for both layers in a tandem device differ from that in a single celled device.[22] An optimum performance for tandem devices is obtained for polymer band gaps of 1.9 eV and 1.5 eV for the front and back device, respectively.[22] In order to study the role of unbalanced transport, both μ_e and μ_h are taken to be the same for both active layers.

Fig. 3 shows the *optimized PCE* of tandem devices with normal or inverted device structures as a function of μ_e/μ_h. In this calculation for every mobility ratio μ_e/μ_h, the layer thicknesses of the front and back device have been optimized for both device geometries. Again the detrimental influence of μ_e/μ_h being unequal to unity on the space charge buildup and the device performance can be observed. The overall trend of the performance is similar to that of the single device with a layer thickness of 100 nm, yet a few differences are present. First of all, each tandem device performs better than its single device counterpart sharing device structure and mobility ratio. Furthermore, the devices with the worst performing device structure having a μ_e/μ_h of 0.001 or 1000 are closer to the performance of their better performing counterparts with the other device structure. For these mobility ratios, the optimum active layers for the front and back devices are very thin [<50 nm], which means that space-charge buildup related losses have far less impact. Here, it is mainly the diminished absorption in the thin layers that limits the attainable device performance. Again for electrons being the slowest charge carriers, the inverted tandem structure yields the best performances. In case of balanced transport, both device geometries perform equally well.

In conclusion, the influence of unbalanced charge transport on the performance of normal and inverted solar cells has been studied by simulations using a combined optical and electrical model. For single cells with a favorable thickness of 250 nm, the normal device structure clearly outperforms the inverted structure for devices with slower hole transport, like most polymer:fullerene devices. It has been shown that this holds as well for tandem devices, assuming that the same mobility ratio is used for both sub-cells.

The authors thank D. J. D. Moet and L. H. Slooff for providing the ellipsometry measurements.

[1]M. A. Green, K. Emery, Y. Hishikawa, and W. Warta, Prog. Photovoltaics **17**, 320 (2009).
[2]Y. Liang, Z. Xu, J. Xia, S. Tsai, Y. Wu, G. Li, C. Ray, and L. Yu, Adv. Mater. **22**, E135 (2010).
[3]M. P. de Jong, L. J. van IJzendoorn, and M. J. A. de Voigt, Appl. Phys. Lett. **77**, 2255 (2000).
[4]K. W. Wong, H. L. Yip, Y. Luo, K. Y. Wong, W. M. Lau, K. H. Low, H. F. Chow, Z. Q. Gao, W. L. Yeung, and C. C. Chang, Appl. Phys. Lett. **80**, 2788 (2002).
[5]J. Gilot, I. Barbu, M. M. Wienk, and R. A. J. Janssen, Appl. Phys. Lett. **91**, 113520 (2007).
[6]P. de Bruin, D. J. D. Moet, and P. W. M. Blom, Org. Electron. **11**, 1419 (2010).
[7]T. J. K. Brenner, I. Hwang, N. C. Greenham, and C. R. McNeill, J. Appl. Phys. **107**, 114501 (2010).
[8]X. W. Sun, D. W. Zhao, L. Khe, A. K. K. Kyaw, G. Q. Lo, and D. L. Kwong, Appl. Phys. Lett. **97**, 053303 (2010).
[9]C.-H. Chou, W. L. Kwan, Z. Hong, L.-M. Chen, and Y. Yang, Adv. Mater. **23**, 1282 (2011).
[10]S. K. Hau, H.-L. Yip, K.-S. Chen, J. Zou, and A. K.-Y. Jen, Appl. Phys. Lett. **97**, 253307 (2010).
[11]D. W. Zhao, L. Ke, S. T. Tan, A. K. K. Kyaw, H. V. Demir, X. W. Sun, D. L. Carroll, G. Q. Lo, and D. L. Kwong, Sol. Energy Mater. **95**, 921, (2011).
[12]J.-C. Wang, W.-T. Weng, M.-Y. Tsai, M.-K. Lee, S.-F. Horng, T.-P. Perng, C.-C. Kei, C.-C. Yu, and H.-F. Meng, J. Mater. Chem. **20**, 862 (2010).
[13]H.-J. Park, K.-H. Lee, B. Humar, K.-S. Shin, S.-W. Jeong, and S.-W. Kim, J. Nanoelectron. Optoelectron. **5**, 1 (2010).
[14]A. A. Pettersson, L. S. Roman, and O. Inganäs, J. Appl. Phys. **86**, 487 (1999).
[15]H. Hoppe, N. Arnold, N. S. Sariciftci, and D. Meissner, Sol. Energy Mater. **80**, 105 (2003).
[16]N.-K. Persson, H. Arwin, and O. Inganäs, J. Appl. Phys. **97**, 034503 (2005).
[17]J. D. Kotlarski, P. W. M. Blom, L. J. A. Koster, M. Lenes, and L. H. Slooff, J. Appl. Phys. **103**, 084502 (2008).
[18]V. D. Mihailetchi, L. J. A. Koster, J. C. Hummelen, and P. W. M. Blom, Phys. Rev. Lett. **94**, 126602 (2004).
[19]L. J. A. Koster, E. C. P. Smits, V. D. Mihailetchi, and P. W. M. Blom, Phys. Rev. B **72**, 085205, (2005).
[20]T. S. Sian and G. B. Reddy, Sol. Energy Mater. Sol. Cells **82**, 375 (2004).
[21]D. R. Lide, *Handbook of Chemistry and Physics* (CRC, Boca Raton, 1994).
[22]J. D. Kotlarski and P. W. M. Blom, Appl. Phys. Lett. **98**, 053301 (2011).
[23]D. Veldman, C. S. J. Meskers, and R. A. J. Janssen, Adv. Funct. Mater. **19**, 1939 (2009).
[24]V. D. Mihailetchi, H. Xie, B. de boer, L. M. Popescu, J. C. Hummelen, P. W. M. Blom, and L. J. A. Koster, Appl. Phys. Lett. **89**, 012107 (2006).
[25]A. Hadipour, B. de Boer, J. Wildeman, F. B. Kooistra, J. C. Hummelen, M. G. R. Turbiez, M. M. Wienk, R. A. J. Janssen, and P. W. M. Blom, Adv. Funct. Mater. **16**, 1897 (2006).
[26]D. J. D. Moet, P. de Bruyn, and P. W. M. Blom, Appl. Phys. Lett. **96**, 153504 (2010).